West Pakistan Water and Power Authority

HYDRAULIC MODEL STUDIES FOR INTAKE STRUCTURES FOR IRRIGATION TUNNELS 3 AND 4

TARBELA DAM PROJECT
INDUS RIVER
WEST PAKISTAN

Prepared for
Tippetts-Abbett-McCarthy-Stratton
New York, New York

by A. G. Mercer

COLORADO STATE UNIVERSITY
ENGINEERING RESEARCH CENTER
CIVIL ENGINEERING DEPARTMENT
FORT COLLINS, COLORADO 80521

August 1970

CER 70-71 AGM9

HYDRAULIC MODEL STUDIES

FOR

INTAKE STRUCTURES FOR IRRIGATION TUNNELS 3 AND 4

AN ADDENDUM TO THE FINAL REPORT OF

HYDRAULIC MODEL STUDIES

FOR

DIVERSION, POWER AND IRRIGATION TUNNELS

January 1965 CER65SSK-JFR6

TARBELA DAM PROJECT

INDUS RIVER

WEST PAKISTAN

Addendum prepared for

Tippetts-Abbett-McCarthy-Stratton

New York, New York

by A. G. Mercer

Colorado State University
Engineering Research Center
Civil Engineering Department
Fort Collins, Colorado 80521

August 1970

CER70-71AGM9

PREFACE

This model study was undertaken by Colorado State University, (CSU) for Tippetts-Abbett-McCarthy-Stratton (TAMS), consulting engineers to the Water and Power Development Authority of West Pakistan (WAPDA), for the Tarbela Project. The work was done at the Engineering Research Center of CSU under the direction of Albert G. Mercer, Associate Professor of Civil Engineering with the help of Allah Rakha and Mohammed Ikramul-Haque, graduate students in Civil Engineering. Grateful acknowledgement is hereby expressed to the shop personnel of the Engineering Research Center for their exceptionally fine work in building the model, and to Karen Helzerman and Kathy Lahmeyer for typing the report.

CONTENTS

FIGURES

LIST OF TABLES

SUMMARY

Hydraulic model studies performed in 1964 of the tunnels for Tarbela Dam were extended to study a revised intake structure for Tunnels 3 and 4. The revision consisted of modifying the intake to accomodate bulkhead gates that could be used, if needed, to dewater the tunnels for maintenance purposes. The studies included observations of the flow for all operating conditions, measurements of piezometric pressures in critical areas to determine cavitation potential and to obtain data for design loads, determination of the form loss coefficient for the intake, measurement of the velocity distribution in the trashracks and observations of the tendency for vortices to form at the entrance to the intake. The intake design performed satisfactorily in the model and design changes appear unnecessary except possibly moderate changes to the central pier to prevent the negative pressures that would occur at certain heads and discharges. The velocity distribution through the trashracks was not as uniform as was expected but a design change to correct this is not recommended here. The model, while somewhat inadequate for proper reproduction of vortices, showed none that would be detrimental to the prototype.

INTRODUCTION

Brief Description of the Project and the Tunnels

The main report[1], to which this is an addendum, describes in some detail the Tarbela Dam Project on the Indus River. Briefly, the dam consists of a main embankment 9000 feet long across the river valley and two auxiliary embankments to close gaps in the left abutment. A service spillway and an auxiliary spillway will be built into the left abutment with a combined capacity of about 1,400,000 cfs at full reservoir level (Elevation 1550). Four tunnels will be provided through the right abutment, as shown in Figure 1, to serve first for diversion and later for power and irrigation releases.

The four tunnels are shown in profile in Figure 2. Tunnels 1 and 2 will first be constructed as diversion tunnels and later converted to power tunnels. The portion of the powerhouse served by Tunnel 1 will be constructed after service as a diversion tunnel has been completed, while that part served by Tunnel 2 will be completed some time in the future. Tunnels 3 and 4 will be constructed in their final form at the start and will be used first as diversion tunnels and later as irrigation release outlets.

The intake structures, as originally planned and as tested in the study described in the main report, did not include provision for closing the tunnels. It was subsequently decided to change the design to provide for bulkheads which could be used to close the tunnels for dewatering if the need arises after the project is completed.

The provision of bulkheads in the intakes of Tunnels 3 and 4 required major changes to the design of the intake structures. Figure 3 shows the geometry of these revised structures. At the upstream end of each tunnel is a trashrack structure with a gross flow area per tunnel of 11,178 square feet, unchanged from the earlier design. Downstream of the trashrack, a central pier has been added. It divides the flow channel into two passages whose cross sectional dimensions converge to 45 feet by 13.5 feet at the location of the bulkheads. The flow area there is 1,215 square feet per tunnel. A short tower with gate slots has been provided for the bulkheads but there is no provision for aeration. The bulkheads will normally be stored elsewhere and will have to be installed below water with barge equipment and divers under conditions of no flow. Downstream of the gate slots, an expanding transition connects the intake to the 45-foot diameter concrete conduit that leads to the tunnel proper. The invert at the intake structure and the concrete conduit is at Elevation 1160 for both tunnels.

The remaining parts of Tunnels 3 and 4 are relatively unchanged from that described in the main report. The upstream portion of each of the tunnels leading to the central gates will be 45 feet in diameter and concrete lined. Each central gate structure has two flow passages, 13.5 feet wide by 45 feet high with transitions upstream and downstream. The portions of the tunnels downstream from the central gate are steel-lined and are 43.5 feet in diameter in Tunnel 3 and 36 feet in diameter in Tunnel 4 (Tunnel 3 has a gradual contraction to 36 feet at the downstream end). Both tunnels are provided with a bifurcation at the downstream end, each leading to two separate contracting sections that connect to the radial gates of the outlet structures. Each of the two gate openings per tunnel are 16 feet wide and 24 feet high with invert at Elevation 1105. The flow area at these gates is 768 sq. ft. per tunnel.

Proposed Operation of Tunnels 3 and 4

River diversion through the tunnels will occur after the wet season during which the final portion of the main embankment is to be completed. The gates of the buttress structure shown in Figure 1 will be lowered, forcing the flow into Tunnels 1 and 2. Tunnels 3 and 4, with higher intakes, will be available as the reservoir level rises during the increased rainy season flows.

As the embankment closure rises, the reservoir will be allowed to fill and the increased head will increase the capacity of the tunnels and the increased storage will reduce the outflows. Tunnels 1 and 2 will be closed as soon as Tunnels 3 and 4 have sufficient head to discharge the outflows by themselves. Judicious operation of the gates in Tunnels 3 and 4 will make possible significant storage of water during the period preceding full completion of the dam.

Scope of the Model Study

The purpose of the model study was to investigate the hydraulic chacacteristics of the revised intake geometry of Tunnels 3 and 4 and to study the hydraulic conditions within the tunnels with the new intakes over the entire range of flows. Specifically, the objectives were to:

1. Observe flow conditions with changes of reservoir operation.

2. Measure piezometric pressure at critical points with the tunnel flowing full with particular attention to potential cavitation areas.

3. Determine the head loss coefficient for the intake.

41 Measure velocity profiles in the trashrack area.

5. Observe possible vortex formation upstream of the trashracks.

Objectives 1 and 2 were to include conditions both with the bulkheads completely removed and also with one passage blocked off.

---

[1] S. Karaki and J. F. Ruff, Hydraulic Model Studies for Diversion, Power and Irrigation Tunnels, Tarbela Dam, Colorado State University, Engineering Research Center, Report No. CER65SSK-JFR6 Fort Collins, Colorado, January 1965.

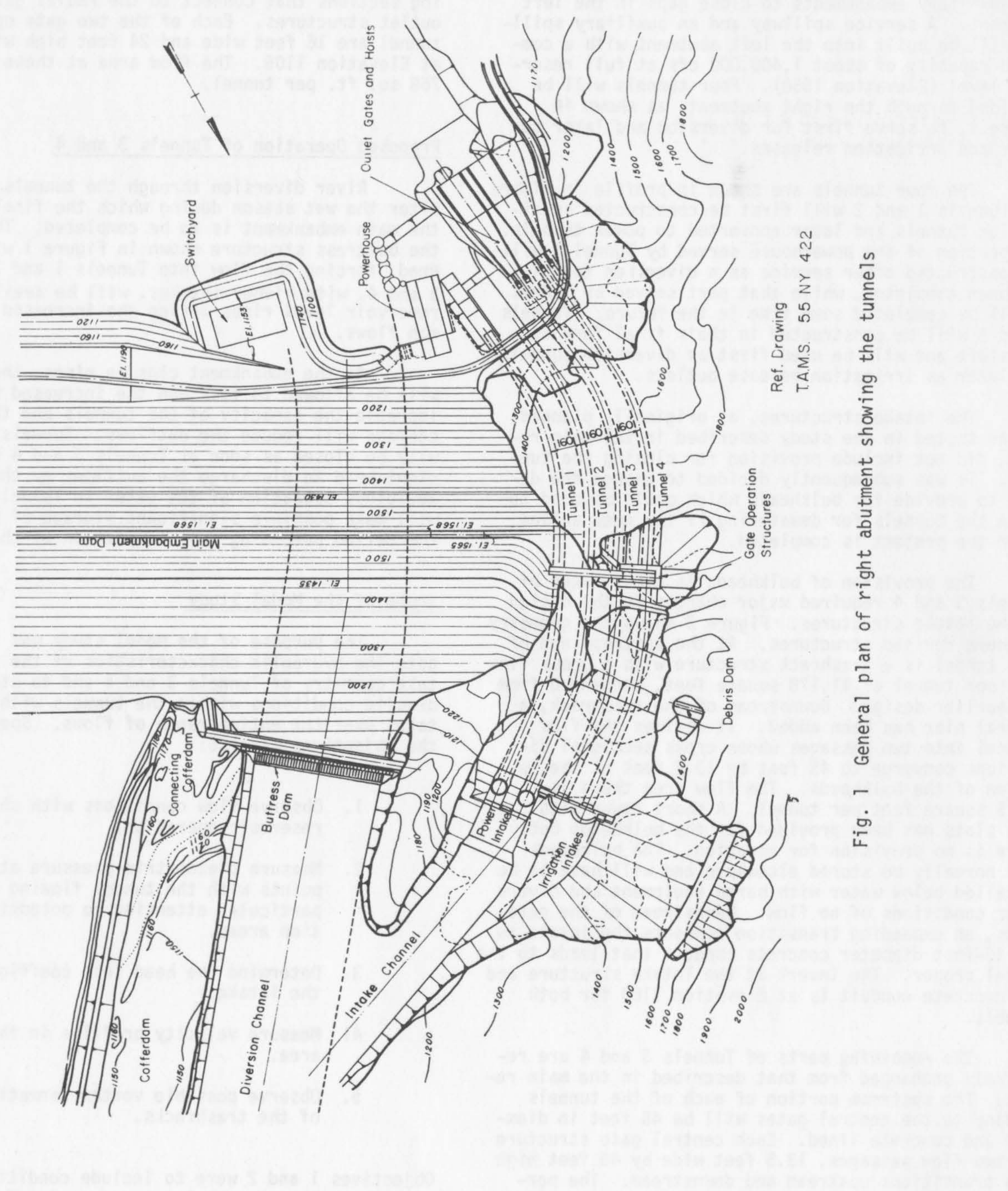

Fig. 1 General plan of right abutment showing the tunnels

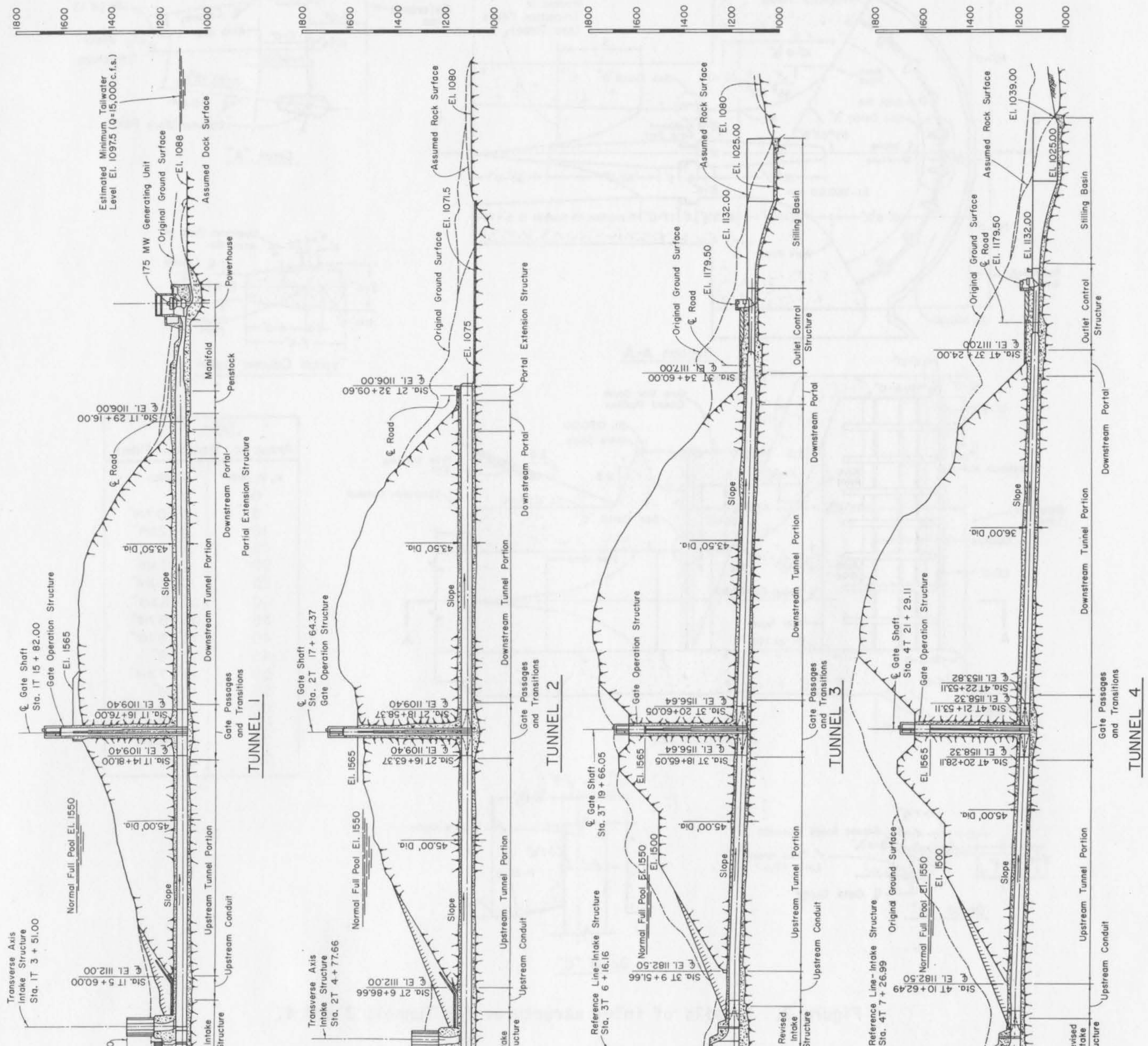

Figure 2. Tunnel profiles.

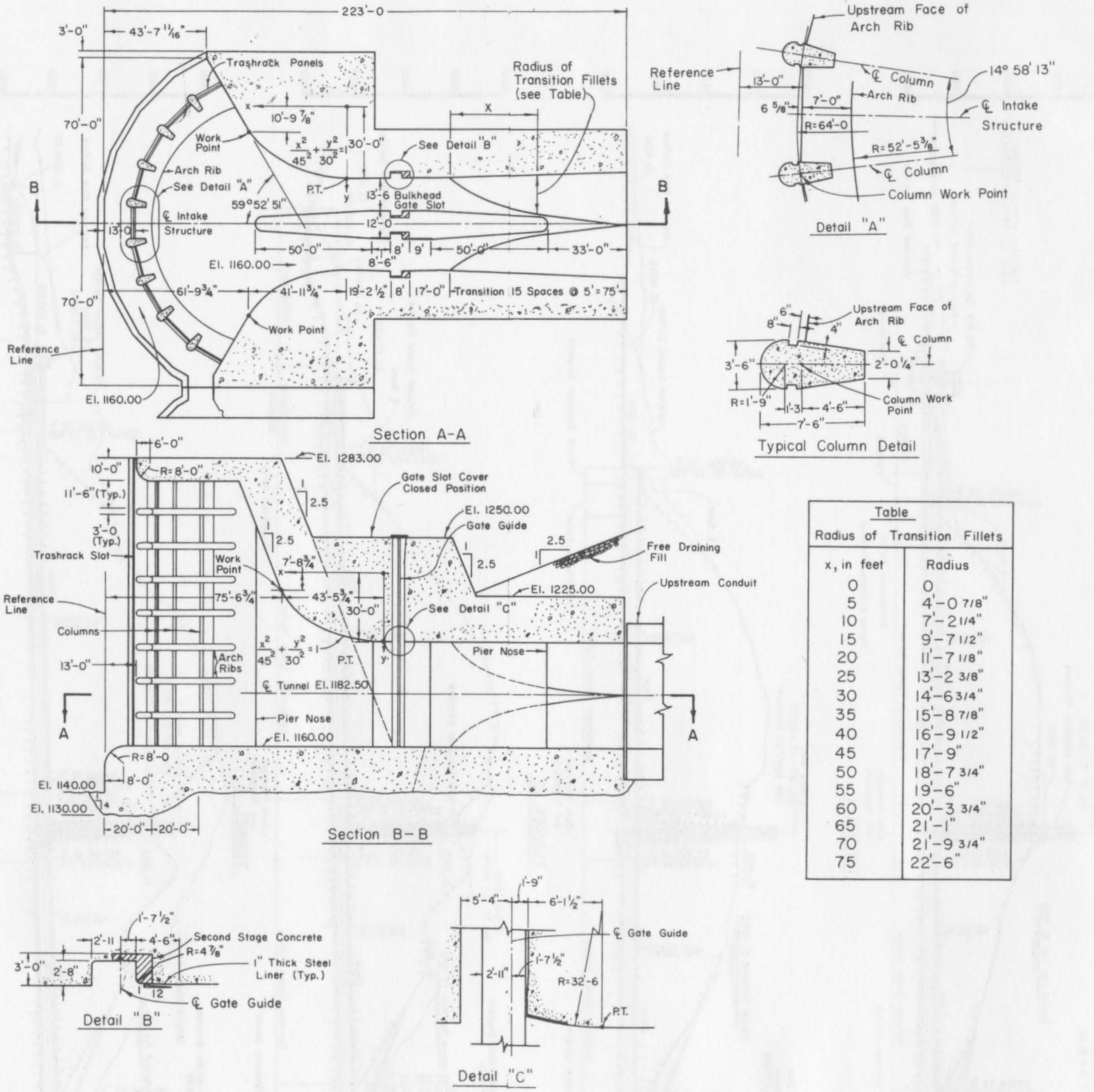

Table	
Radius of Transition Fillets	
x, in feet	Radius
0	0
5	4'-0 7/8"
10	7'-2 1/4"
15	9'-7 1/2"
20	11'-7 1/8"
25	13'-2 3/8"
30	14'-6 3/4"
35	15'-8 7/8"
40	16'-9 1/2"
45	17'-9"
50	18'-7 3/4"
55	19'-6"
60	20'-3 3/4"
65	21'-1"
70	21'-9 3/4"
75	22'-6"

Figure 3. Details of inlet structures for Tunnels 3 and 4.

II. DESCRIPTION OF THE MODEL

The model was arranged to make use of as many of the parts of the model used in the earlier tunnel study as possible. A schematic of the model layout is shown in Figure 4 and the actual model is pictured in Figure 5 viewed from the area of the weir box. The model reproduced the geometry of Tunnel 3 from the intake structure to about 300 feet downstream of the centerline of the central gate operation structure. The remaining part of Tunnel 3 was not reproduced because any effect this portion would have on the intake structure could be simulated by an artificial obstruction at the end of the model. The differences between Tunnels 3 and 4 in the section reproduced are relatively minor so that results obtained from the Tunnel 3 geometry are readily adaptable to Tunnel 4.

The model length scale ratio was, of course, the same as used earlier, 1:69.6. With the model operating according to the Froude number, the scale ratios for velocity, etc., are given in Table 1.

TABLE I
MODEL-PROTOTYPE SCALE RATIOS

Parameter	Scale Ratio		Absolute Magnitudes	
	Function of the Length	Numerical Ratio	Prototype	Model
Length	L_r	1:69.6	1 ft	0.172 in.
Velocity	$L_r^{1/2}$	1:8.343	1 ft/sec	0.120 ft/sec
Discharge	$L_r^{5/2}$	1:40413	100,000 cfs	2.474 cfs

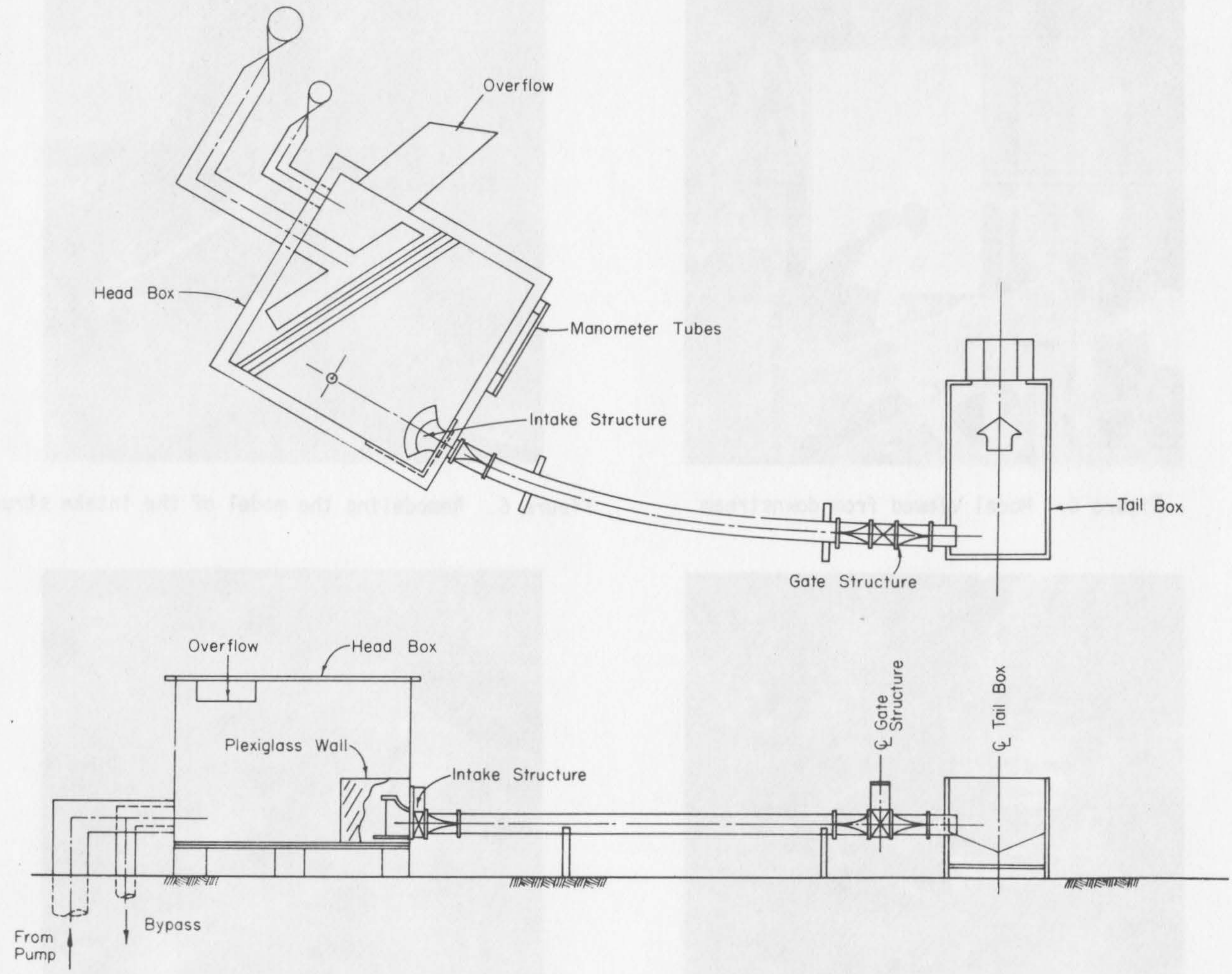

Figure 4. General arrangement of the model.

As before, no adjustments were made to the length or slope of the model tunnel to compensate for differences between model and prototype friction factors.

It was possible to make use of existing model hardware for virtually all of the model parts. Only the intake structure and the transition immediately downstream required modification. The intake structure was completely disassembled and reassembled according to the new configuration. Fortunately, the basic contours were not altered and the original pieces were re-used with the necessary adjustments. New templates, such as those shown in Figure 6, were cut to insure that the close tolerances of the original model were maintained. New pieces of plastic were machined for the central pier (see Figure 7) and the section of the intake containing the gate tower and slots.

The original wooden core used to form the plastic downstream transition was available and it was reworked to the new dimensions (see Figure 8). Since the inner dimensions for the modified transition were smaller than for the original, the modification was made by inserting the reshaped core into the original model and filling the gap caused by the difference in dimensions with an epoxy based material. This produced a transition with opaque walls, as shown in Figure 9, but with very good dimensional reproduction. Figure 10 shows the completed model.

A total of 80 piezometer taps were installed in the intake structure and downstream transition, located as shown in Figure 11. These, in addition to 6 piezometer taps already existing in the tunnel section, are listed in Table 2 along with their location in terms of elevation and of distance from the main reference line at the upstream end of the intake. The photograph of Figure 10 shows the model with piezometer taps installed.

III. ANALYTICAL FLOW STUDIES

Analytical studies were made with the help of a computer to determine the effect, if any, that the downstream porti n of the tunnel would have on the flow upstream. A computer program was developed to compute the flow depths all along both tunnels for different discharge rates. Friction losses were computed from Manning's equation using an "n" value of .014. In addition it was assumed that each of the

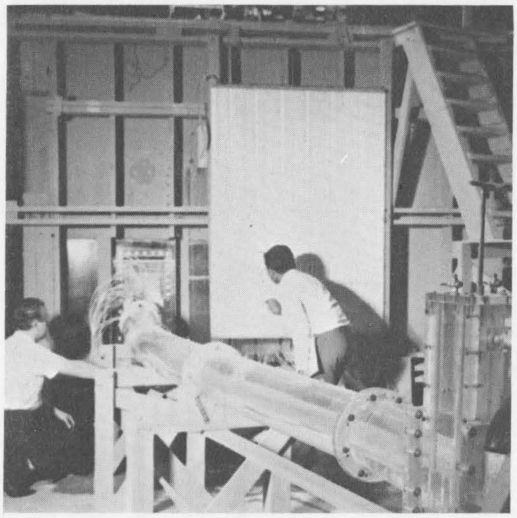

Figure 5. Model viewed from downstream

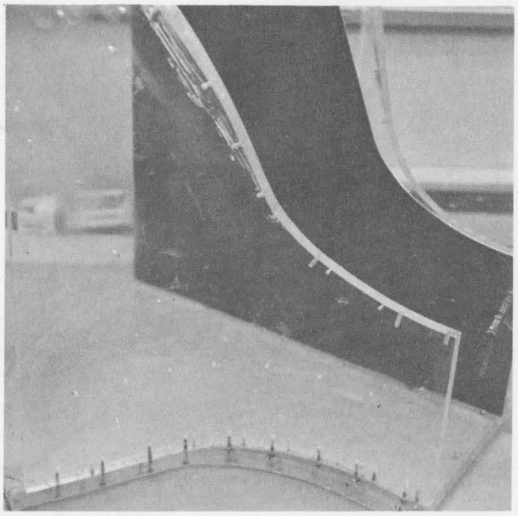

Figure 6. Remodeling the model of the intake structure

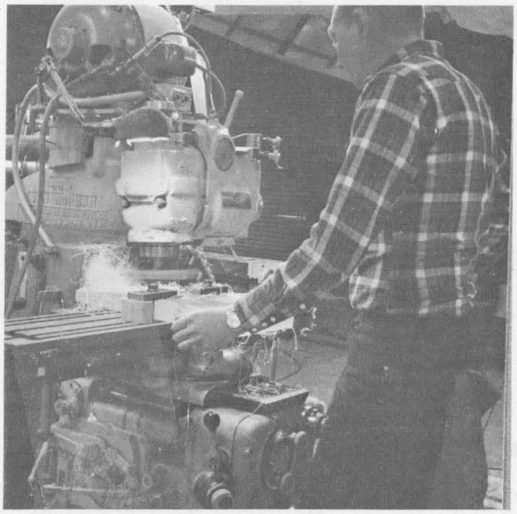

Figure 7. Machining the central pier

Figure 8. Modifying the wooden core for the downstream transition

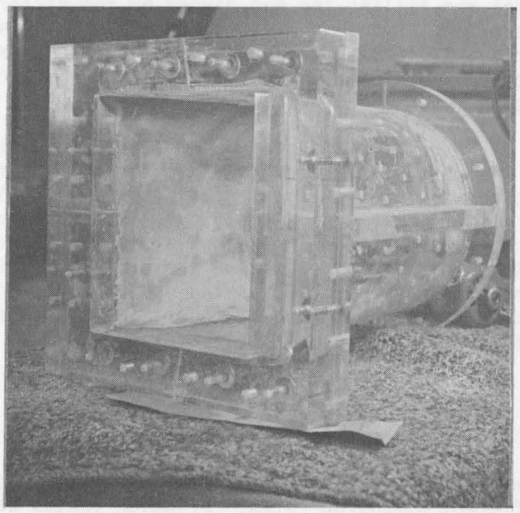

Figure 9. Modified downstream transition

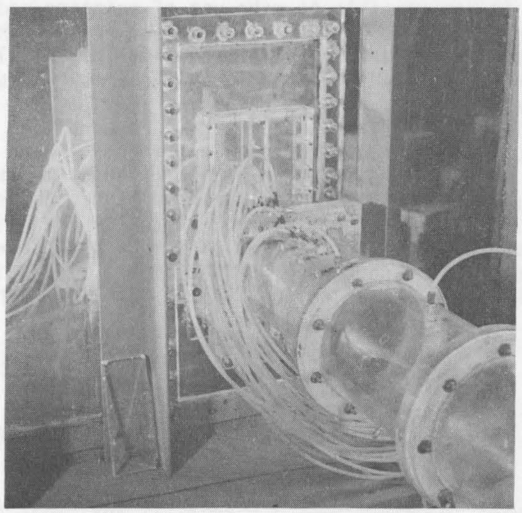

Figure 10. Closeup of the intake model with piezometer taps installed

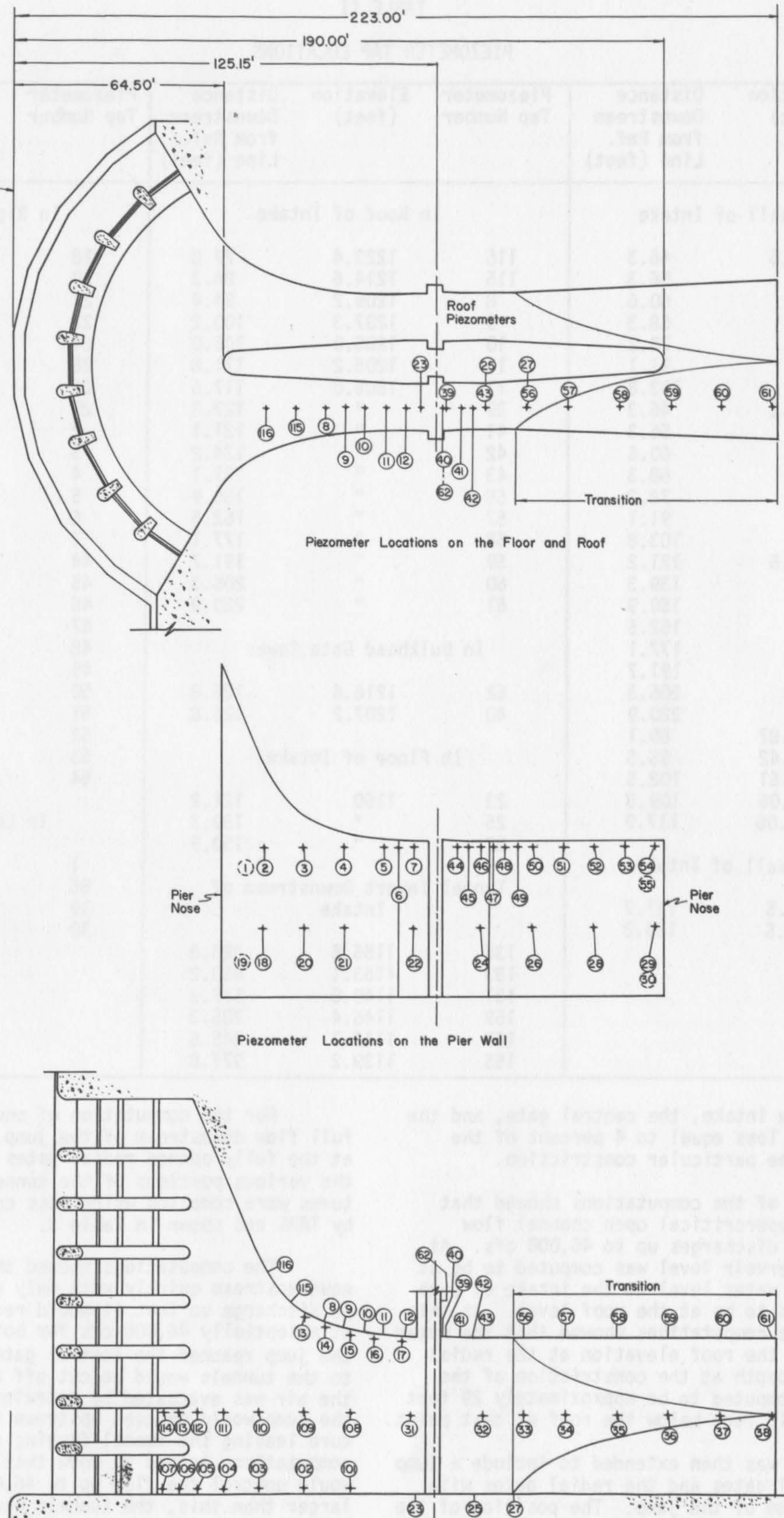

Figure 11. Piezometer locations in the intake structure

TABLE II

PIEZOMETER TAP LOCATIONS

Piezometer Tap Number	Elevation (feet)	Distance Downstream from Ref. Line (feet)
In Right Side Wall of Intake		
107	1161.5	46.3
106	"	56.3
105	"	60.6
104	"	68.3
103	"	78.2
102	"	91.1
101	"	103.8
114	1183.2	46.3
113	"	56.3
112	"	60.6
111	"	68.3
110	"	78.2
109	"	91.1
108	"	103.8
31	1182.5	121.2
32	"	139.3
33	"	150.9
34	"	162.5
35	"	177.1
36	"	191.7
37	"	206.3
38	"	220.9
13	1210.87	89.1
14	1209.42	95.5
15	1206.51	102.5
16	1205.06	109.5
17	1205.06	117.9
In Left Side Wall of Intake		
63	1182.5	121.2
64	1182.5	139.3

Piezometer Tap Number	Elevation (feet)	Distance Downstream from Ref. Line (feet)
In Roof of Intake		
116	1223.4	77.8
115	1214.6	84.3
8	1209.2	94.4
9	1207.3	100.2
10	1205.0	106.0
11	1205.2	111.8
12	1205.0	117.6
39	"	127.3
41	"	131.1
42	"	134.2
43	"	137.1
56	"	150.9
57	"	162.5
58	"	177.1
59	"	191.7
60	"	206.3
61	"	220.9
In Bulkhead Gate Tower		
62	1216.6	126.8
40	1207.2	126.8
In Floor of Intake		
23	1160	121.2
25	"	139.3
27	"	150.9
Tunnel Invert Downstream of Intake		
135	1156.5	320.8
133	1153.1	450.2
131	1149.8	577.3
159	1146.4	705.3
157	1142.7	845.5
155	1139.2	977.8

Piezometer Tap Number	Elevation (feet)	Distance Downstream from Ref. Line (feet)
In Right Wall of Pier		
18	1179.6	75.2
20	"	86.8
21	"	98.4
22	"	118.8
24	"	136.9
26	"	152.2
28	"	169.6
29	"	187.1
2	1203.5	75.2
3	"	86.8
4	"	98.4
5	"	110.0
6	"	114.4
7	"	118.8
44	"	129.7
45	"	133.3
46	"	136.9
47	"	140.6
48	"	144.2
49	"	147.8
50	"	152.2
51	"	160.9
52	"	169.6
53	"	178.4
54	"	187.1
In Left Wall of Pier		
1	1203.5	75.2
55	"	187.1
19	1179.6	75.2
30	"	187.1

constrictions: the intake, the central gate, and the exit caused a head loss equal to 4 percent of the velocity head at the particular constriction.

The results of the computations showed that both tunnels had supercritical open channel flow throughout for all discharges up to 46,000 cfs. At this flow, the reservoir level was computed to be at Elev. 1225 and the water level at the intake of each tunnel was computed to be at the roof level. At this same discharge, the computations showed that the water was also very near the roof elevation at the radial gates. The water depth at the constriction of the central gate was computed to be appxoximately 29 feet for both tunnels, 16 feet below the roof at that point.

The program was then extended to include a jump between the central gates and the radial gates with full flow downstream of the jump. The position of the jump was established by the computer by comparing the difference in energy levels in the part full flow upstream and in the full flow downstream, considering the losses across the jump as determined by momentum principles.

For the computation of energy contained in the full flow downstream of the jump, control was assumed at the fully opened radial gates and losses through the various portions of the tunnels and their structures were computed using loss coefficients supplied by TAMS and shown in Table 3.

The computations showed that the jump would move upstream quickly with only a very small increase in discharge so that it would reach the central gates at essentially 46,000 cfs for both tunnels. Once the jump reached the central gates the supply of air to the tunnels would be cut off and, as quickly as the air was evacuated by entrainment in the jump, the jump would proceed upstream to the intake structure leaving the tunnel flowing completely full. The computations served to show that the intake structure would control the flow up to 46,000 cfs and, for flows larger than this, the tunnels would flow full with control at the downstream radial gates. The results of the model studies, however, revealed that the prototype tunnels' behavior would be somewhat different than indicated above. These results are described below.

TABLE III

LOSS COEFFICIENTS FOR TUNNELS 3 AND 4 ACCORDING TO TAMS

STRUCTURE	AREA SELECTED FOR LOCAL SECTION (sq. ft.)	LOSS COEFFICIENT IN TERMS OF local velocity head	velocity head at exit
Tunnel 3			
Concrete lined tunnel	1590	.208	.0484
Bend	1590	.027	.0063
Central gate structure	1486	.340	.0910
Steel lined tunnel	1486	.221	.0592
Bend	1486	.048	.0129
Reducer to 36' diameter	1018	.040	.0228
Bifurcation and transitions	768	.160	.1600
Exit	768	1.000	1.0000
Tunnel 4			
Concrete lined tunnel	1590	.218	.0508
Bend	1590	.027	.0063
Central gate structure	1018	.140	.0798
Steel lined tunnel	1018	.327	.1870
Bend	1018	.044	.0249
Bifurcation and transitions	768	.160	.1600
Exit	768	1.000	1.0000

IV. MODEL TESTS AND RESULTS

Description of the Flow

The flow in the model was observed over the full range of reservoir water levels for conditions with both intake passages open and also with one passage closed by a bulkhead gate. Data on discharge and reservoir levels were taken for the case with both passages open and the results are presented in Figure 12. This data was not taken for single passage operation as it is not a planned mode of operation and would only occur if removal of one bulkhead gate were physically impossible for some reason.

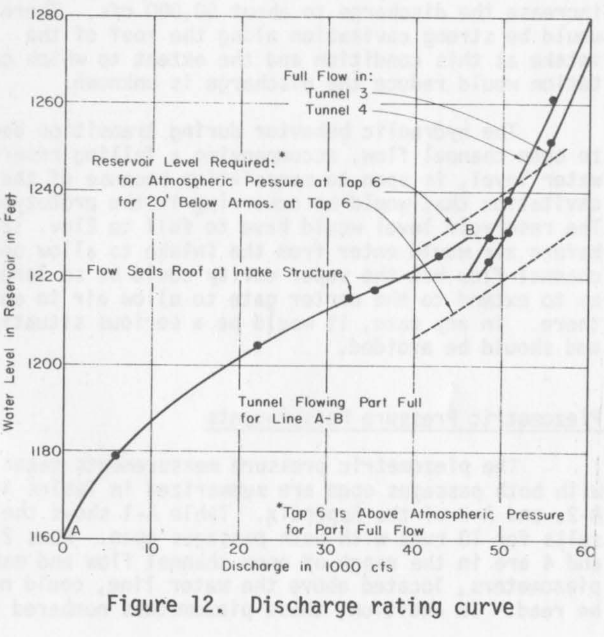

Figure 12. Discharge rating curve

For reservoir water levels below Elev. 1215 (discharges less than 32,600 cfs) the model shows there would be open channel, supercritical flow all along the tunnel with discharge control at the intake. Since the intakes of Tunnels 3 and 4 are essentially identical, the discharge rating curve for this range of reservoir levels is the same for both. When the reservoir level reaches Elev. 1215, the water level in the intake touches the roof and seals off the upstream end of the tunnel. However, air can still enter the tunnel from downstream so that open channel flow persists in the tunnel and control for higher reservoir levels remains at the intake.

Figure 13 shows the water surface profile along the tunnel with 32,600 cfs flowing and the reservoir water level at Elev. 1215. Although the water level touches the roof at the entrance to the intake, the level at the gate slots is approximately eight feet below the roof. This level is in good agreement with the analytical study which did not foresee the water touching the roof at the converging section upstream of the gate slots at this relatively low flow and thus predicted upstream priming at the higher flow of 46,000 cfs.

The flow through the intake structure is very regular and steady and is free from unusual surface disturbances or turbulence generating separations. The depth in the 45-foot diameter tunnel for this flow varies from about 22 feet at the end of the intake transition to approximately 20 feet just upstream of the central gate structure. The flow through the central gate is characterized by rather large oblique waves and disturbances, but the average depth is approximately 26 feet.

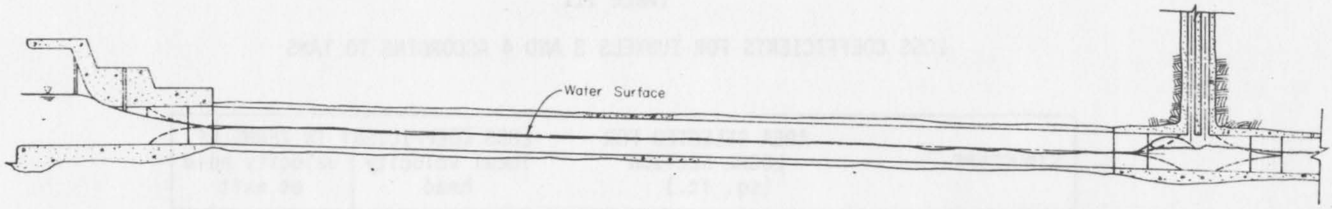

Figure 13. Water surface profile for 32,600 cfs

The transition from open channel flow to full flow had to be initiated artificially in the model because the exit structure was not reproduced. According to the previously discussed analytical studies this transition would occur in the prototype at a flow of 46,000 cfs. To simulate this in the model an adjustable gate was attached to the exit of the model and with the reservoir water level set at Elev. 1229.5 (which produces a flow of 46,000 cfs under intake control), the gate was slowly lowered until a jump formed in the tunnel. The jump was then allowed to move upstream through the central gate structure to close off the supply of air from the aerators there. Without further adjustment of the exit gate, the tunnel was observed to fill completely by evacuating the air through entrainment in the jump. This process is considered to have reproduced the expected prototype behavior very closely and the model showed that the transition would occur very smoothly with no surging or "belching" of air.

With the tunnel flowing full there was very little to observe but it was noticed that the thin walled plastic pipe representing the tunnel had, when touched, no appreciable vibration anywhere along its length indicating a minimum of large scale turbulence.

To obtain the discharge rating curves for full flow, shown in Figure 12, the exit gate was adjusted to maintain the pressure at Piezometer Tap 155, located in the tunnel invert, at levels shown in Figure 14.

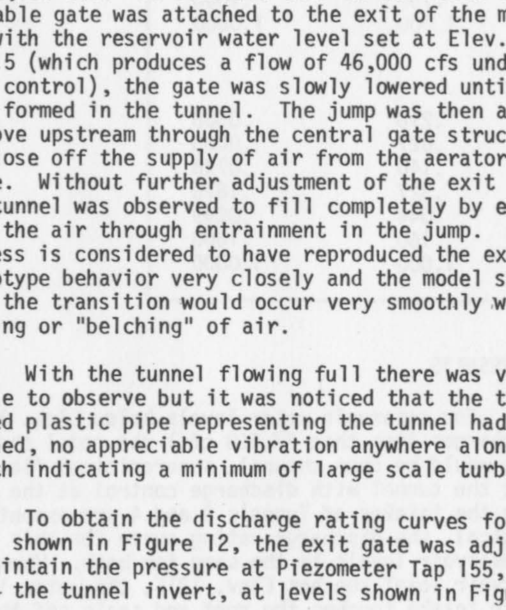

Figure 14. Pressures in the tunnel at Tap 155 needed to simulate the control by the radial gates

These values were obtained analytically using the TAMS data of Table 3. The discharge rating curves for full flow differ, of course, for Tunnels 3 and 4 because of friction differences throughout the different sized tunnels.

The discharge rating curves for falling reservoir levels are different than for rising levels in the discharge range covering the transition from full to part full flow. With the reservoir levels falling, the tunnel remains full down to approximately Elev. 1220, at which level air starts to enter along the roof of the intake. This air collects immediately downstream of the intake creating near atmospheric pressure there so that the control switches to the intake with a resulting decrease in discharge. With the discharge reduced, the hydraulic jump downstream of the air pocket is swept fairly slowly out of the tunnel. The action appears regular and is not accompanied by excessive surging.

Observations were also made with one intake passage closed by a bulkhead gate. The flow in the model follows the same general pattern as with both passages open but, as will be discussed later, pressures which would be subatmospheric in the prototype occurred over a wide range of flows. If both the central and radial gates were fully open and one of the intake passages were closed, there would be open channel flow throughout the tunnel until the reservoir water level reached about Elev. 1220 (20,000 cfs flow) and the tunnel sealed at the intake. Open channel flow would continue downstream of the intake until the reservoir water level reaches about Elev. 1300 (46,000 cfs discharge) and the hydraulic jump from downstream reaches the intake. The transition to full flow would increase the discharge to about 50,000 cfs. There would be strong cavitation along the roof of the intake at this condition and the extent to which cavitation would reduce the discharge is unknown.

The hydraulic behavior during transition back to open channel flow, accompanying a falling reservoir water level, is open to speculation because of the cavitation that would be occurring in the prototype. The reservoir level would have to fall to Elev. 1220 before air would enter from the intake to allow open channel flow but the vapor cavity could be so large as to extend to the center gate to allow air to enter there. In any case, it would be a serious situation and should be avoided.

Piezometric Pressure Measurements

The piezometric pressure measurements taken with both passages open are summarized in Tables A-1, A-2, and A-3 of the Appendix. Table A-1 shows the results for 10 runs with both passages open. Runs 2, 3 and 4 are in the range of open channel flow and many piezometers, located above the water line, could not be read. In addition, those piezometers numbered above 100 were not connected. The area of potential cavitation was covered, however, and all readings taken indicated pressures above atmospheric except for several taps lying near the water surface which indicated pressures approximately 3 feet below atmospheric. It would appear from this that no potential cavitation areas exist under conditions of open channel flow. The maximum velocity through the intake under these conditions would be approximately 53 fps.

The remaining seven runs were for full tunnel flow. Runs 5, 6, 7 and 10 were made with only those piezometers numbered below 100 connected. Runs 14, 15 and 16 were added to include the piezometers numbered above 100 along with some of those under 100 retained for a check. The discharges for all of the full flow runs are in slight disagreement with TAMS head losses of Table 3 because these values were not available at the time. However, the method of analysis used for pressure does not require close agreement. The piezometer pressures of Table A-1 are reduced to pressure coefficients in Table A-2. This coefficient is the result of subtracting the piezometric head from the reservoir water level and dividing the difference by the velocity head in the 45-foot diameter tunnel.

Table A-2 shows that the pressure coefficient is a constant (within experimental error) for each piezometer tap even though the reservoir levels range from Elev. 1245 to Elev. 1525 and discharges range from 64,000 cfs to 112,000 cfs. The average pressure coefficient for each tap, covering all runs, is also given in Table A-2. These average values, which range from nearly zero to 2.342 for Tap 6 on the wall of the center pier, are shown plotted on Figures 15, 16, and 17. High values of pressure coefficient, which plot towards the bottom of the figures, correspond to low pressures and high velocities. This form of presenting pressure data has the advantage of being dimensionless and being applicable to all reservoir water levels and discharges. Actual pressures can be obtained for any condition by a simple calculation.

Figure 15 shows the average pressure coefficient on the walls of the center pier. The pressure gradient for the contracting flow upstream of the gate guide is clearly shown as is the partial pressure recovery downstream. The theoretical pressure coefficient at the gate guides, considering one-dimensional flow and ignoring friction, is 1.715, somewhat higher than the values shown. The pressure coefficients for the taps near the top of the wall (Elev. 1203.5) are generally higher than those lower down. The highest pressure coefficient (Tap 6) occurs at the point where the upstream taper joins the parallel throat section, just upstream of the gate slots. This point is the junction of two flat surfaces which should possibly be transitioned in the prototype to obtain a lower pressure coefficient at that point.

The significance of the pressure coefficient at Tap 6 is shown by the two oblique broken lines in Figure 12. The upper one shows, as a function of reservoir water level, the discharges that would produce atmospheric pressure at Tap 6. The lower one shows the discharges that would produce a pressure head 20 feet below atmospheric pressure at Tap 6. The implication of these curves is that the area near Tap 6 will be below atmospheric pressure when the tunnel is flowing full and the reservoir is below Elev. 1245. As indicated before, this does not hold true when the tunnel is flowing part full, nor would it be true if the radial gates were partially closed to reduce the tunnel flow.

The pressure coefficients on the inlet roof and invert are shown in Figure 16 and on the walls of the inlet structure in Figure 17. They show the same general trend as the pressure coefficients of Figure 15, especially the trend for the pressure coefficients to be highest (actual piezometric pressures to be lowest) near the roof of the intake.

The pressures taken with the left passage of the intake structure closed are tabulated in Table A-3 in the Appendix. This mode of operation, although it should never occur, would be a critical one for loading on the central pier. The pressures were taken mainly for use in determining the loading. Cavitation considerations are secondary. The piezometer taps numbered greater than 100 were not available for these tests, but none of the 100 series are located on the central pier. Open channel flow existed for Run 13 but the flow for Runs 11 and 12 filled the tunnel. Piezometric heads are tabulated for all these runs and pressure coefficients are shown for Runs 11 and 12 and for the average of the two. The average pressure coefficients are shown plotted in Figures 18, 19 and 20.

The pressure coefficients on the center pier are plotted on Figure 18. This figure is comparable to Figure 15 except that the pressure coefficient scale is four times larger. The position of the plotted points for the right wall are very much the same in both figures. Tap 6 is still the highest with an average pressure coefficient of 9.14. The pressure coefficients for the left wall are shown to be essentially zero upstream of the closed gate and 5.90 downstream. The pressure coefficients for the roof and invert are shown in Figure 19 and those for the intake structure walls are shown in Figure 20.

While cavitation is a secondary consideration for single gate operation it should be realized that the pressure coefficients indicate that there would be very severe and widespread cavitation in the intake for reservoir water levels up to the order of Elev. 1350 if the tunnel is flowing full and the downstream gates are open.

Form Loss Coefficient

The piezometer taps located in the invert of the tunnel downstream of the intake structure were used to determine the form loss coefficient for the intake. The piezometric heads measured in the model for these piezometers are tabulated in Table A-1, along with those for the other intake piezometers, and the pressure coefficients are presented in Table A-2. The pressure coefficients for the tunnel are plotted in Figure 21 according to their location relative to the downstream end of the transition to the circular section. The straight line that best fits the data is also shown. This line represents, in a dimensionless form, the hydraulic grade line for the tunnel. From this line the value of the pressure coefficient at the beginning of the tunnel can be read off and this value is 1.320. Since this represents in dimensionless form the sum of the velocity head in the tunnel plus the form loss, it follows that the form loss coefficient will be less by unity or 0.320. This is, of course, based on tunnel velocity.

The slope of the hydraulic grade line can be used to obtain the value of Manning's "n" for the tunnel. The value that is obtained for "n" is 0.0158. Manning's "n" is not dimensionless and this value is based on prototype rather than model dimensions.

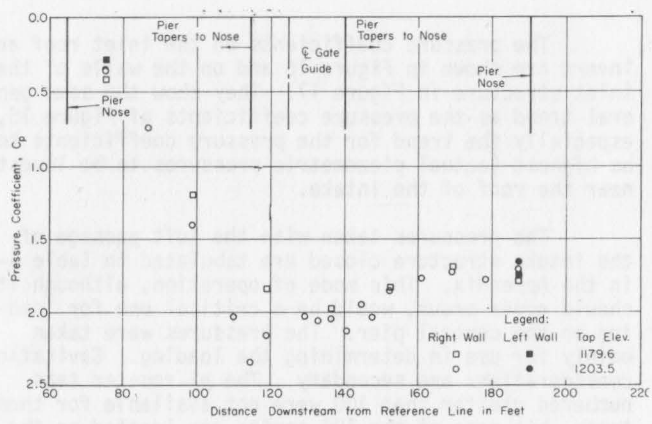

Figure 15. Average pressure coefficients on center pier with both passages open

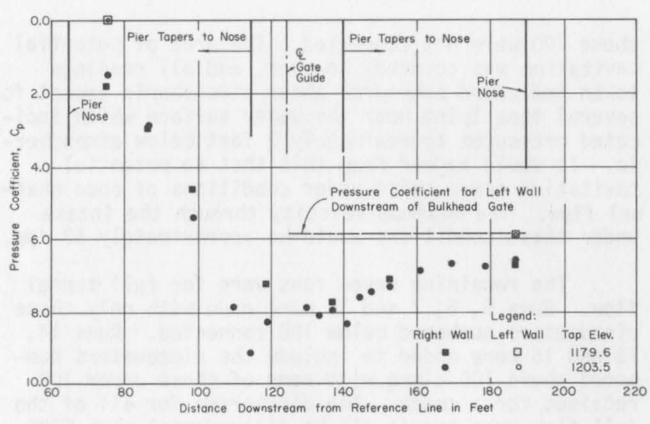

Figure 18. Average pressure coefficients on center pier with left passage closed

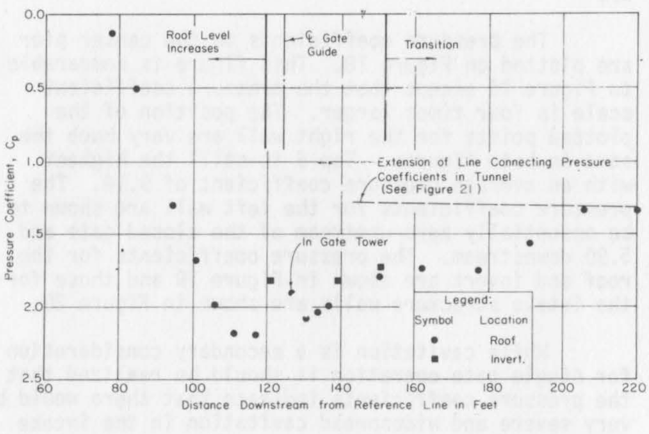

Figure 16. Average pressure coefficients on roof and invert with both passages open

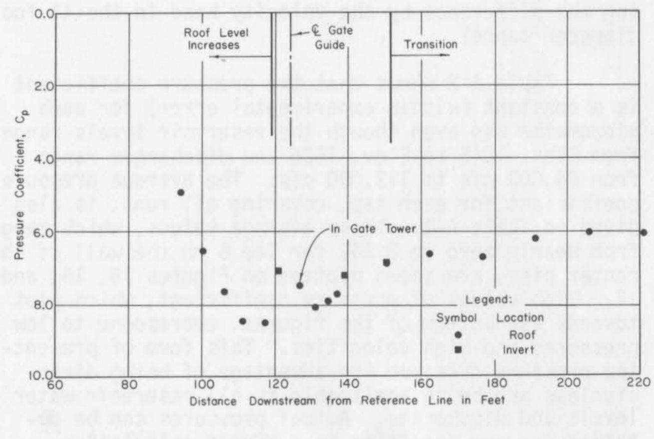

Figure 19. Average pressure coefficients on roof and invert with left passage closed

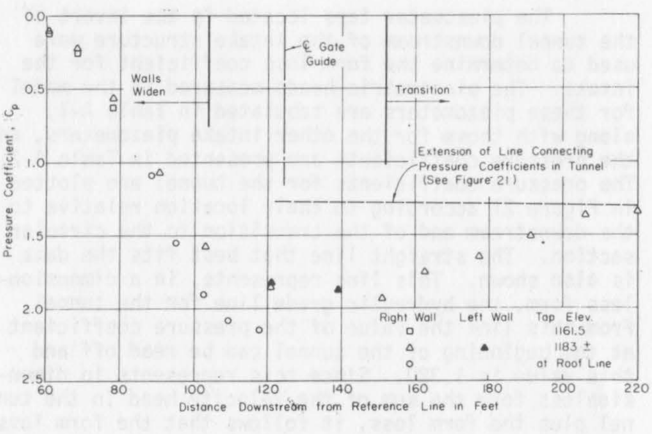

Figure 17. Average pressure coefficients on intake structure walls with both passages open

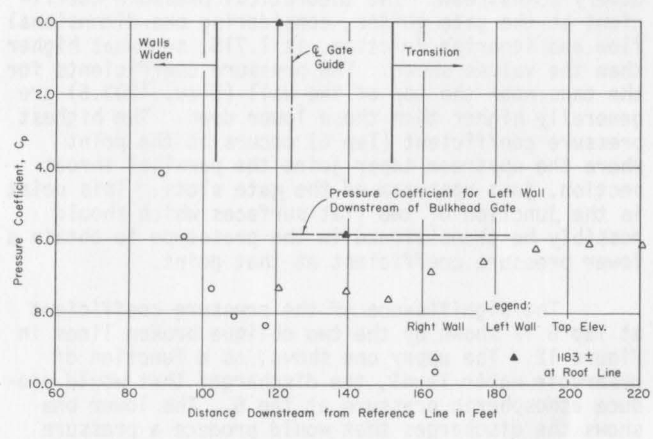

Figure 20. Average pressure coefficients on intake structure walls with left passage closed

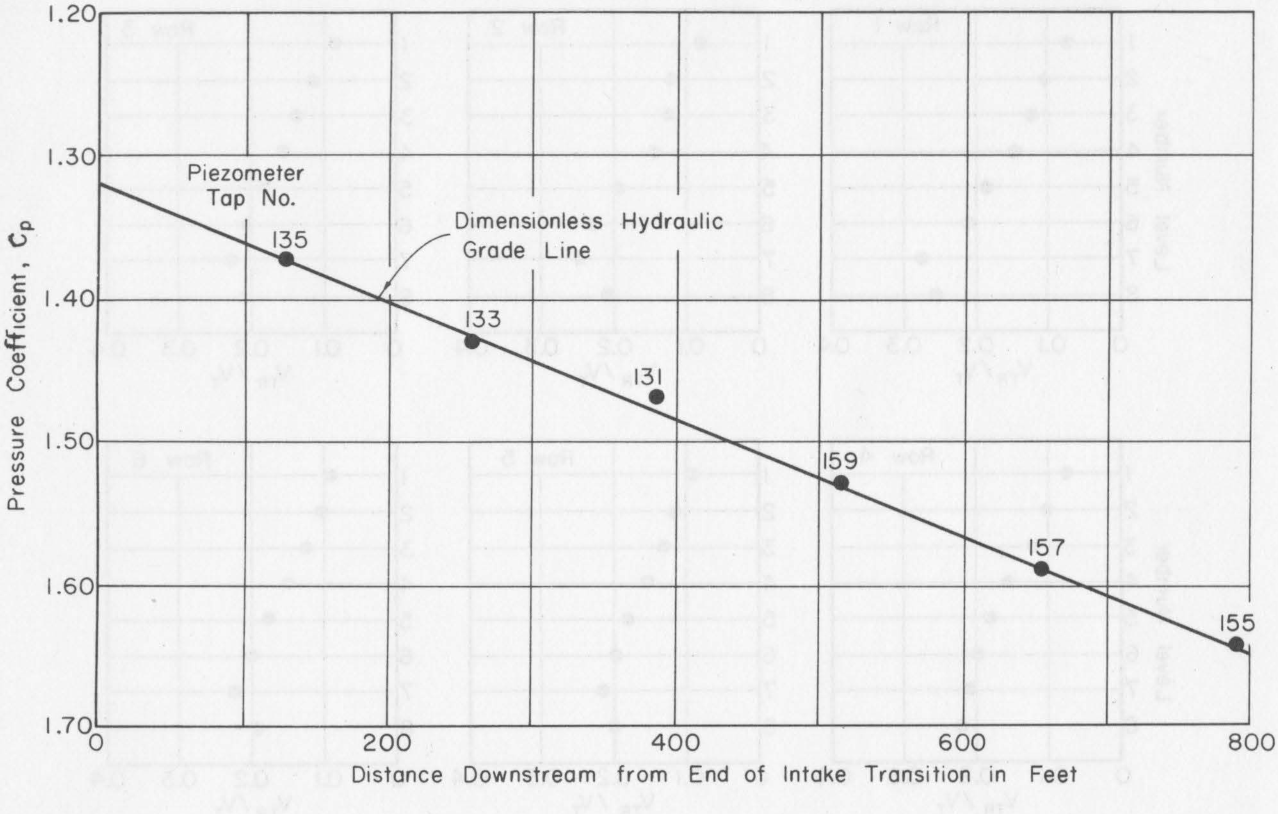

Figure 21. Average pressure coefficients along tunnel invert

This value also includes, however, the extra losses that may result from the bend in the tunnel.

Trashrack Velocities

Velocities in the trashrack area were measured with a propellor-type velocity meter and the results are presented in Table A-4 of the Appendix. The trashrack columns and the arch ribs were reproduced in the model but not the trashrack panels themselves. Velocity readings were taken in the center of each of the squares of the grid formed by the ribs and columns. The data in Table A-4 are for two runs, both with the tunnel flowing full but with different reservoir levels and discharge. To extend this data to include all possible discharges the ratio of measured velocity to tunnel velocity were computed for each measurement. The dimensionless velocities for both runs compared within experimental error, indicating that the reservoir water level has little effect on the velocity distribution. The average velocity ratios for the two runs are shown in Table A-4 and also plotted in Figure 22. In this figure the row numbers refer to the vertical rows of square openings between trashrack columns, counting from the right. The level numbers refer to the horizontal rows of square openings between rib arches, counting from the top.

The velocity profiles for each of the vertical rows of openings are very similar and show a progressive decrease in velocity towards the top of the intake. The dimensionless velocities range from 0.076 to 0.279 as compared with 0.142 which is the theoretical value for the uniform flow through the trashracks. The reason for this nonuniform velocity pattern is that the flow approaches the trashrack horizontally near the bottom and flows smoothly over the arched ribs while the flow approaches obliquely downwards near the top and suffers more losses from the ribs. The solution, if it were feasible, would be to have the trashrack sloped rather than vertical.

Vorticity at the Intake

Visual observations were made of vorticity immediately upstream of the intake, but before the results are presented, a few comments should be made regarding the phenomena. The vortices commonly observed in the eddy regions of rivers, such as downstream of bridge piers, and the vortices that occur in the intake flow of tunnels appear the same but their mechanics of formation are quite different.

All vortices result from rotational flow. In eddy regions (gate slots are an example) the rotation develops and grows right in the eddy itself as a

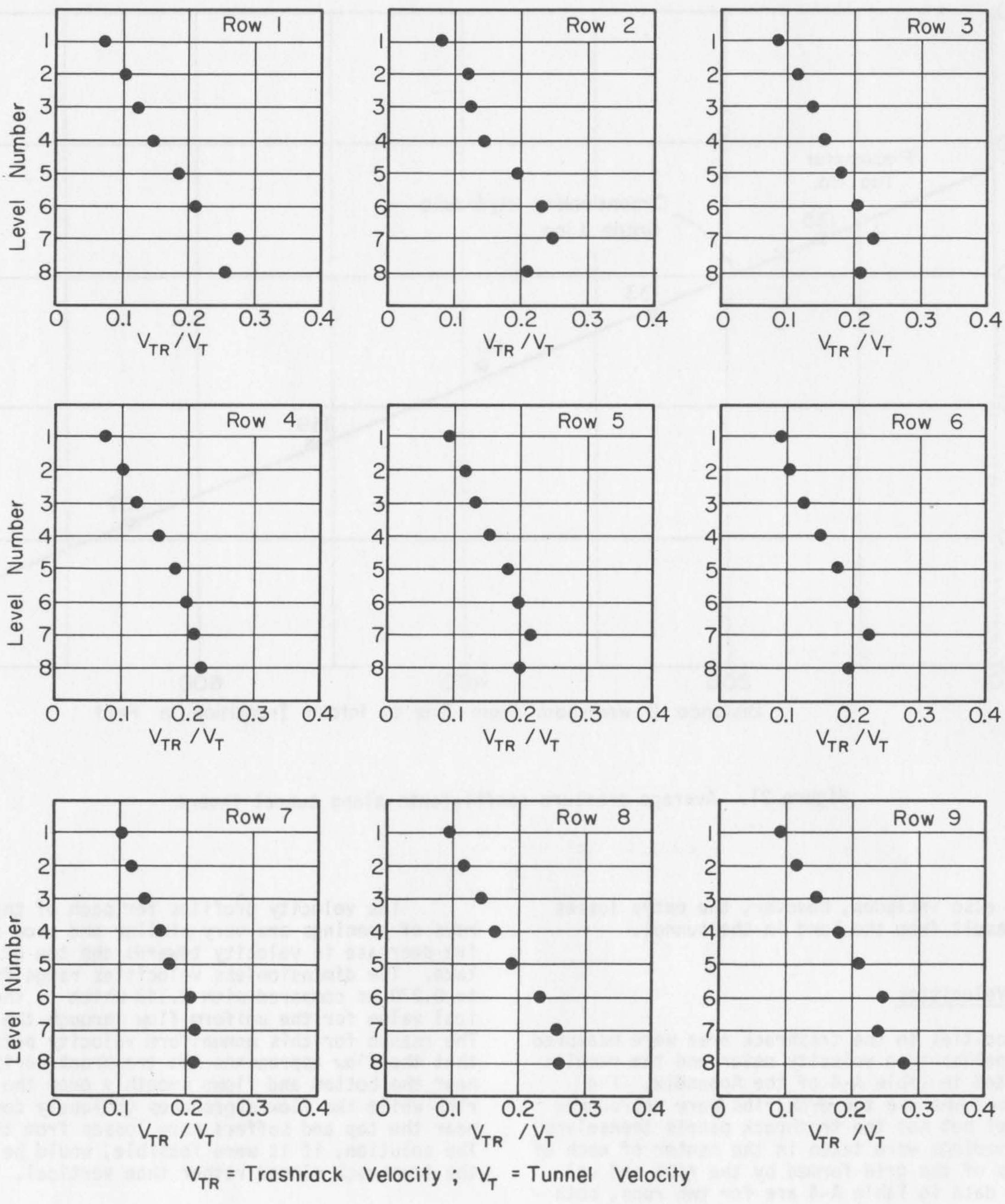

Figure 22. Trashrack velocities

result of both the local geometry and the local flow. This type of eddy is very consistent and is well reproduced even in models of moderate size. The type of eddy that develops in intakes (bathtub drain eddies are an example) are the result of a concentration at the intake of pre-existing rotation. The rotational component of the flow contributing to the vortex is generated some distance upstream of the inlet, usually by wall friction, not at the inlet itself or in the tunnel downstream. To model this type of vortex reliably, the approach flow must be reproduced for some distance upstream in order to generate the necessary amount of rotation in the incoming flow. The local geometry is important, of course, because it determines how the rotation is concentrated and where the vortex will form. The strength of the vortex and the sense of rotation, however, is largely a function of the upstream geometry. With good upstream representation a moderate sized model will give fair quantitative reproduction of intake vortices.

In the present model the upstream conditions are not modeled so that the vortices are not entirely reliable. They represent only the combination of the rotation producing properties of the model head box and the concentrating properties of the intake. The observations were made, nevertheless, and the results are described below.

According to hydrodynamic theory, the centerline of a vortex muxt extend unbroken throughout the fluid or until it terminates on a boundary surface. The usual termination of an intake vortex is the water surface upstream of the intake, although some geometries cause the termination to occur on the bed of the approach channel. In the present model they definitely terminated on the water surface and observations of the flow patterns on the surface were sufficient to detect all vortices.

Observations of the flow patterns on the reservoir water surface upstream of the intake were made with the water surface set initially at a high level and then allowed to fall slowly. Discharge was maintained according to computations applicable when the radial gates are full open and control is at the exit.

No vortices were observed until the reservoir level reached Elev. 1299. At that level a definite counterclockwise vortex developed immediately upstream of the intake and just left of center. At its maximum strength the vortex caused the water level at its center to be depressed only about 0.1 inch and an air core was never formed. This vortex persisted intermittently until the reservoir dropped to Elev. 1280 when smaller vortices developed above each of the trashrack columns to replace it. The depressions at the center of these vortices were too small to measure. Below Elev. 1273 the reservoir water level is lower than the roof of the intake and, as would be expected, all vortices vanish. At lower elevations very small vortices do appear at the left and right edge of the intake. These are of the wake or separation type and are probably accurately represented as they will occur in the prototype but they are much too small to have any detrimental consequence.

V. CONCLUSIONS

The intake structure performs satisfactorily when both passages are open for operation both with and without the tunnel flowing full. The transition from part full flow to full flow and the transition from full flow to part full flow, as reproduced in the model, occur smoothly without excess surging or the discharging of large slugs of air.

The piezometric pressures are near atmospheric pressure or above for all flow conditions except on the central pier upstream of the gate slot. The design could be improved by providing a smoother transition between the tapered sections of the pier and the untapered section, both upstream and downstream of the gate slots.

The flow pattern with one passage closed is satisfactory but the piezometric pressures throughout the intake indicated that severe cavitation will occur for full tunnel flow. This condition is a direct function of the cross-sectional area of the single passage and cannot be corrected by simple design change.

The velocities through the lower parts of the trashracks are as high as twice the nominal velocity due to a strong downward component to the flow restricting flow through upper parts of the trashrack.

The model was not extensive enough to properly reproduce intake vortices so that no really meaningful conclusions can be made regarding them. Those that were observed in the model, however, were too small to be judged detrimental to the flow.

APPENDIX

Table A-1	Piezometric heads with both passages open
Table A-2	Coefficients of pressure based on tunnel velocity for full tunnel flow
Table A-3	Piezometric heads and pressure coefficients for bulkhead closing one side of intake
Table A-4	Velocities at the trashracks

TABLE A-1

PIEZOMETRIC HEADS WITH BOTH PASSAGES OPEN

Run Number	2	3	4	10	16	7	15	6	14	5
H.W.L. (feet)	1204.4	1215.6	1234.2	1245.6	1253.6	1310.0	1364.4	1390.0	1517.0	1525.7
Discharge*(cfs)	22,300	32,600	49,900	66,800	70,900	70,400	63,900	87,600	101,300	112,000
Piezometer Number	Piez. Head	Piez. Head	Piez. Head	Piez. Head	Piez. Head	Piez. Head	Piez. Head	Piez. Head	Piez. Head	Piez. Head
107					1252.0		1362.3		1512.6	
106					1250.9		1362.0		1512.0	
105					1249.4		1360.9		1508.8	
104					1245.2		1357.4		1500.1	
103					1235.5		1347.8		1474.2	
102										
101										
114					1252.2		1362.3		1513.2	
113					1251.3		1362.3		1512.0	
112					1249.8		1361.2		1510.6	
111					1246.3		1358.0		1502.7	
110					1236.1		1349.8		1481.2	
109					1220.5		1337.0		1449.0	
108					1205.1		1324.5		1416.4	
31	1192.5	1201.0	1204.0	1194.6		1253.9		1301.6		1382.4
32	1185.0	1188.0	1200.1	1193.7		1252.7		1299.8		1378.9
33	1184.5	1193.8	1197.7	1192.4		1251.6		1297.5		1374.5
34	1184.4	1192.4	1197.9	1197.2		1258.8		1306.2		1389.4
35			1195.5	1200.4		1260.0		1310.9		1397.5
36			1193.6	1204.2		1264.4		1314.9		1409.1
37			1191.2	1207.7		1268.4		1324.3		1419.3
38			1187.7	1208.6		1269.3		1325.4		1420.8
13			1218.1	1216.3		1276.7		1336.8		1439.1
14			1211.2	1203.6		1262.9		1315.8		1404.8
15			1205.6	1193.7		1252.1		1298.0		1377.5
16			1203.1	1188.8		1246.9		1290.5		1363.8
17			1202.9	1186.5	1187.0	1244.6	1310.3	1286.5	1512.0	1357.4
63	1186.8	1201.3	1204.9	1195.5		1284.8		1333.3		1414.4
64	1183.3	1197.1	1201.4	1193.7		1283.3		1330.4		1409.5
116					1250.1		1360.0		1509.1	
115					1238.1		1351.0		1484.4	
8			1214.9	1210.7		1270.8		1328.0		1425.1
9			1208.7	1199.5		1259.7		1309.7		1394.3
10			1204.2	1191.5		1250.1		1295.2		1371.6
11			1201.7	1186.2		1244.6		1286.4		1356.8
12			1203.1	1186.0		1244.0		1285.6		1355.1
39				1192.6		1252.1		1299.8		1380.9
41				1188.9		1247.5		1291.7		1364.6
42				1189.9		1248.7		1293.4		1368.4
43				1191.1		1250.1		1295.8		1372.2
56				1197.1		1256.2		1304.8		1387.9
57				1199.1		1257.4		1307.4		1392.0
58				1198.2		1257.1		1306.8		1390.8
59				1203.3		1262.6		1315.8		1405.9
60				1208.3		1269.0		1325.1		1420.5

* see note 5

Run Number	2	3	4	10	16	7	15	6	14	5
H.W.L. (feet)	1204.4	1215.6	1234.2	1245.6	1253.6	1310.0	1364.4	1390.0	1517.0	1525.7
Discharge*(cfs)	22,300	32,600	49,900	66,800	70,900	70,400	63,900	87,600	101,300	112,000
Piezometer Number	Piez. Head	Piez. Head	Piez. Head	Piez. Head	Piez. Head	Piez. Head	Piez. Head	Piez. Head	Piez. Head	Piez. Head
61				1209.1		1269.3		1326.0		1421.9
62				1195.5		1251.0		1290.2		1364.1
40				1188.2		1246.3		1289.4		1362.3
23	1192.3	1200.6	1203.9	1195.8	1197.9	1285.1	1318.4	1333.3	1402.7	1415.0
25	1189.4	1197.3	1201.2	1195.3	1197.6	1284.5	1318.1	1332.4	1402.2	1412.7
27	1188.5	1196.4	1201.7	1196.9	1199.4	1289.4	1320.5	1339.4	1405.3	1424.3
135					1211.2		1329.5		1431.0	
133					1209.2		1328.0		1427.7	
131					1208.0		1326.9		1424.8	
159					1206.1		1325.4		1420.8	
157					1204.2		1324.0		1417.6	
155					1202.6		1322.8		1414.4	
18	1201.6	1212.0	1227.2	1234.1	1240.9	1297.2	1353.9	1369.6	1490.5	1492.8
20	1200.1	1209.9	1222.2	1224.8	1230.8	1287.0	1345.6	1353.9	1468.5	1467.0
21	1197.5	1209.0	1215.1	1212.8	1219.2	1273.7	1334.3	1332.4	1431.4	1431.8
22	1192.0	1201.1	1204.0	1194.6	1196.9	1253.9	1318.2	1302.2	1401.3	1383.3
24	1189.0	1196.9	1199.4	1191.1	1192.7	1250.1	1319.4	1295.8	1392.3	1372.5
26	1186.5	1194.3	1199.0	1195.5	1197.3	1254.5	1318.2	1302.7	1402.6	1384.1
28				1198.7	1201.0	1258.3	1321.3	1308.2	1409.7	1393.1
29	1178.4	1180.6	1186.2	1196.1	1198.7	1255.9	1319.3	1303.9	1403.6	1385.0
2			1228.8	1236.2		1299.5		1373.0		1498.1
3			1222.9	1225.3		1287.3		1354.2		1467.0
4			1215.1	1207.2		1267.0		1322.5		1416.7
5			1203.6	1189.9		1248.7		1293.7		1369.3
6			1200.4	1181.8		1239.4		1278.6		1343.7
7			1203.3	1186.5		1244.6		1287.9		1359.7
44				1189.9		1249.0		1294.6		1369.6
45				1189.1		1247.8		1292.0		1365.5
46				1189.9		1248.4		1293.1		1367.6
47				1187.6		1246.0		1288.2		1359.7
48				1192.6		1251.3		1297.2		1375.4
49				1190.8		1248.7		1292.0		1365.5
50				1194.7		1253.3		1299.8		1378.6
51				1197.8		1256.8		1305.6		1387.9
52				1198.9		1258.0		1308.0		1394.0
53				1197.8		1255.9		1304.5		1386.8
54				1199.8	1200.7	1257.4	1321.3	1307.4	1410.1	1392.9
1			1228.8	1236.0	1242.3	1295.9	1355.4	1372.5	1493.8	1497.2
55				1200.4	1202.7	1259.1	1322.8	1310.3	1414.4	1399.5
19	1203.3	1213.7	1230.6	1236.9	1244.3	1301.3	1357.0	1377.2	1500.6	1505.6
30	1178.5	1180.9	1187.3	1197.5	1200.0	1257.1	1320.5	1306.5	1407.1	1395.8

Notes:

1) Open channel flow in model for Runs 2, 3, 4
2) Full tunnel flow in model for Runs 10, 16, 7, 15, 6, 14, 5
3) Only piezometer taps numbered 2 through 65 connected up for Runs 2, 3, 4, 10, 7, 6, 5
4) Only piezometer taps numbered 1, 17 through 30, 54, 55 and 101 and higher connected for Runs 16, 15, 14
5) Discharge and H. W. L. were set for convenience of obtaining pressure measurements and do not necessarily agree with the tunnel rating curves
6) Piezometer locations shown in Table 2 and Fig. 10

TABLE A-2

COEFFICIENTS OF PRESSURE BASED ON TUNNEL VELOCITY
FOR FULL TUNNEL FLOW

Run Number	10	16	7	15	6	14	5	
H.W.L. (feet)	1245.6	1253.6	1310.0	1364.4	1390.0	1517.0	1525.7	
Discharge (cfs)	66,800	70,900	70,400	63,900	87,600	101,300	112,000	
Piezometer Number	Pres. Coef.	Pres. Coef.	Pres. Coef.	Pres. Coef.	Pres. Coef.	Pres. Coef.	Pres. Coef.	Avg. Pres. Coef.
107		.05		.07		.07		.063
106		.09		.08		.08		.083
105		.12		.13		.13		.127
104		.27		.26		.27		.267
103		.58		.64		.68		.633
102								
101								
114		.05		.07		.06		.060
113		.07		.07		.08		.073
112		.12		.11		.10		.110
111		.23		.24		.23		.237
110		.56		.56		.57		.563
109		1.06		1.07		1.08		1.070
108		1.55		1.56		1.60		1.570
31	1.86		1.84		1.88		1.86	1.860
32	1.89		1.88		1.91		1.91	1.897
33	1.94		1.92		1.96		1.96	1.945
34	1.77		1.75		1.78		1.77	1.767
35	1.65		1.64		1.68		1.67	1.660
36	1.51		1.50		1.53		1.51	1.512
37	1.38		1.37		1.40		1.38	1.382
38	1.35		1.34		1.37		1.36	1.355
13	1.07		1.10		1.13		1.12	1.105
14	1.54		1.55		1.57		1.57	1.557
15	1.89		1.90		1.93		1.92	1.910
16	2.08		2.07		2.11		2.10	2.090
17	2.16	2.15	2.15	2.15	2.20	2.15	2.19	2.167
63	1.82		1.81		1.84		1.84	1.827
64	1.90		1.86		1.90		1.90	1.890
116		.11		.15		.13		.130
115		.49		.52		.52		.510
8	1.27		1.29		1.31		1.31	1.295
9	1.68		1.65		1.70		1.71	1.685
10	1.98		1.97		2.01		2.00	1.990
11	2.17		2.15		2.20		2.19	2.178
12	2.17		2.17		2.21		2.22	2.192
39	1.93		1.90		1.91		1.88	1.905
41	2.07		2.05		2.09		2.09	2.075
42	2.04		2.01		2.05		2.04	2.035
43	1.99		1.97		2.00		1.99	1.988
56	1.77		1.77		1.81		1.79	1.785
57	1.70		1.73		1.75		1.74	1.730
58	1.73		1.74		1.77		1.75	1.748
59	1.55		1.57		1.57		1.56	1.562
60	1.36		1.35		1.38		1.37	1.365

Run Number	10	16	7	15	6	14	5	
H.W.L. (feet)	1245.6	1253.6	1310.0	1364.4	1390.0	1517.0	1525.7	
Discharge (cfs)	66,800	70,900	70,400	63,900	87,600	101,300	112,000	
Piezometer Number	Pres. Coef.	Pres. Coef.	Pres. Coef.	Pres. Coef.	Pres. Coef.	Pres. Coef.	Pres. Coef.	Avg. Pres. Coef.
61	1.33		1.34		1.36		1.35	1.345
62	1.83		1.94		2.12		2.10	1.998
40	2.10		2.09		2.13		2.12	2.110
23	1.82	1.80	1.81	1.83	1.84	1.81	1.83	1.820
25	1.84	1.81	1.82	1.84	1.86	1.82	1.86	1.836
27	1.79	1.75	1.66	1.74	1.71	1.77	1.71	1.733
135		1.37		1.38		1.37		1.373
133		1.43		1.44		1.42		1.430
131		1.47		1.48		1.46		1.470
159		1.53		1.53		1.53		1.530
157		1.59		1.60		1.58		1.590
155		1.65		1.65		1.63		1.643
18	.42	.41	.42	.42	.43	.42	.43	.421
20	.76	.74	.75	.75	.77	.77	.76	.757
21	1.20	1.18	1.19	1.20	1.22	1.20	1.22	1.201
22	1.86	1.83	1.84	1.84	1.86	1.84	1.85	1.846
24	1.99	1.97	1.97	1.99	2.00	1.98	1.99	1.984
26	1.83	1.82	1.82	1.84	1.85	1.82	1.84	1.831
28	1.71	1.70	1.70	1.71	1.73	1.70	1.72	1.710
29	1.81	1.77	1.78	1.79	1.83	1.80	1.83	1.787
2	.35		.34		.36		.37	.355
3	.74		.74		.76		.76	.750
4	1.40		1.40		1.43		1.42	1.412
5	2.04		2.01		2.04		2.03	2.030
6	2.33		2.32		2.36		2.36	2.342
7	2.16		2.15		2.17		2.18	2.165
44	2.04		2.00		2.02		2.03	2.025
45	2.07		2.04		2.08		2.08	2.067
46	2.04		2.02		2.05		2.05	2.040
47	2.12		2.10		2.16		2.16	2.135
48	1.94		1.93		1.97		1.95	1.947
49	2.00		2.01		2.08		2.08	2.042
50	1.86		1.86		1.91		1.91	1.885
51	1.75		1.75		1.79		1.79	1.770
52	1.72		1.71		1.74		1.71	1.720
53	1.75		1.78		1.81		1.80	1.785
54	1.67	1.71	1.73	1.71	1.75	1.68	1.73	1.711
1	.36	.36	.36	.35	.37	.37	.37	.363
55	1.65	1.65	1.67	1.65	1.69	1.63	1.67	1.658
19	.32	.30	.29	.28	.27	.27	.26	.284
30	1.75	1.73	1.74	1.74	1.77	1.74	1.69	1.738

Notes:

1) Coefficients of pressure are for data of Table A-1
2) The coefficient of pressure is obtained by subtracting the piezometric head from the reservoir elevation and dividing the result by the velocity head in the main tunnel

TABLE A-3

PIEZOMETRIC HEADS AND PRESSURE COEFFICIENTS

Bulkhead Closing One Side of Intake

Run Number	13	12	11	12	11	
H.W.L. (feet)	1255.3	1249.0	1528.9	1249.0	1528.9	
Discharge (cfs)	33,000	34,300	69,000	34,300	69,000	
Piezometer Number	Piez. Head	Piez. Head	Piez. Head	Pres. Coef.	Pres. Coef.	Avg. Pres. Coef.
31	1204.8	1196.1	1317.9	7.32	7.22	7.27
32	1200.0	1195.2	1312.6	7.44	7.39	7.41
33	1194.8	1193.6	1305.4	7.67	7.64	7.66
34	1196.6	1199.5	1329.5	6.85	6.82	6.84
35	1192.7	1201.6	1334.1	6.56	6.66	6.61
36	1191.1	1204.0	1345.5	6.22	6.27	6.25
37	1188.7	1204.9	1350.4	6.09	6.10	6.10
38	1183.8	1204.8	1349.2	6.11	6.14	6.12
13	1227.2	1219.3	1407.7	4.11	4.14	4.13
14	1215.4	1206.1	1356.8	5.93	5.88	5.90
15	1206.1	1195.6	1314.7	7.39	7.33	7.36
16	1201.7	1190.4	1294.0	8.11	8.03	8.07
17	1201.3	1187.7	1285.0	8.47	8.34	8.40
63		1248.4	1527.2	.08	.07	.08
64		1205.6	1360.3	6.00	5.76	5.88
8	1222.1	1213.4	1383.8	4.92	4.96	4.94
9	1211.5	1201.7	1338.2	6.54	6.52	6.53
10	1204.2	1193.4	1304.5	7.69	7.67	7.68
11	1199.8	1187.8	1282.4	8.47	8.43	8.45
12	1202.2	1187.4	1280.1	8.51	8.51	8.51
39		1193.8	1308.2	7.63	7.54	7.58
41		1190.6	1293.1	8.07	8.06	8.06
42		1191.3	1297.8	7.98	7.90	7.94
43		1192.6	1303.6	7.80	7.70	7.75
56		1198.7	1327.4	6.94	6.86	6.90
57		1200.3	1335.0	6.73	6.63	6.68
58		1199.8	1332.4	6.80	6.72	6.76
59		1204.1	1345.7	6.20	6.26	6.23
60		1205.2	1352.5	6.05	6.03	6.04
61		1204.8	1350.7	6.12	6.09	6.10
62		1190.0	1290.8	8.16	8.14	8.15
40		1189.5	1291.1	8.22	8.13	8.18
23	1204.7	1197.4	1321.9	7.13	7.08	7.10
25	1199.7	1196.7	1318.7	7.25	7.19	7.22
27	1199.5	1198.7	1327.7	6.95	6.88	6.92
18	1243.1	1235.9	1476.3	1.81	1.80	1.80
20	1234.8	1227.4	1441.7	2.99	2.98	2.98
21	1223.2	1215.2	1393.1	4.66	4.64	4.65
22	1204.8	1196.6	1318.7	7.24	7.19	7.22
24	1197.4	1192.6	1302.7	7.80	7.73	7.78
26	1198.1	1197.1	1321.1	7.18	7.11	7.14
28	1193.7	1200.2	1334.1	6.74	6.66	6.70
29	1170.5	1200.5	1329.8	6.71	6.81	6.76
2	1245.6	1238.7	1486.3	1.42	1.46	1.44
3	1235.8	1228.0	1443.6	2.90	2.92	2.91
4	1218.7	1209.6	1370.9	5.45	5.40	5.42
5	1203.3	1191.7	1299.7	7.91	7.84	7.88
6	1196.5	1183.4	1259.9	9.07	9.20	9.14
7	1202.4	1188.6	1287.0	8.36	8.27	8.32
44		1191.7	1298.7	7.93	7.87	7.90
45		1190.5	1294.3	8.09	8.02	8.06
46		1191.4	1297.2	7.96	7.92	7.94
47		1188.8	1286.5	8.33	8.29	8.31
48		1193.8	1307.7	7.63	7.56	7.60
49		1191.1	1306.2	7.33	7.60	7.46
50		1196.2	1313.8	7.30	7.36	7.33
51		1199.4	1326.9	6.87	6.91	6.89
52		1200.7	1330.9	6.69	6.77	6.73
53		1200.6	1327.7	6.69	6.88	6.79
54		1200.8	1337.9	6.66	6.53	6.60
1	1255.2	1249.0	1528.6	.00	.01	.00
55		1205.9	1359.7	5.95	5.78	5.87
19	1254.8	1248.9	1528.0	.02	.03	.02
30		1205.4	1359.1	6.03	5.80	5.90

TABLE A-4

VELOCITIES AT THE TRASHRACKS

Row Number	Level Number	Trashrack Vel. in fps	Trashrack Vel. in fps	$\frac{V_{tr}}{V_t}$	$\frac{V_{tr}}{V_t}$	Average V_{tr}/V_t
Run Number		20	21	20	21	
Discharge in cfs *		89,000	105,000			
H.W.L. in feet		1290	1430			
Tunnel Velocity in fps		56	66			
1	1	4.6	4.6	.082	.070	.076
	2	5.6	7.8	.100	.118	.109
	3	6.6	8.8	.118	.134	.126
	4	8.0	10.1	.143	.153	.148
	5	10.3	12.5	.184	.189	.186
	6	11.0	14.0	.213	.213	.213
	7	15.9	17.5	.283	.265	.274
	8	13.4	17.5	.238	.265	.252
2	1	4.5		.080		.080
	2	7.0		.124		.124
	3	7.0		.126		.126
	4	8.2		.147		.147
	5	10.8		.193		.193
	6	12.8		.229		.229
	7	13.8		.246		.246
	8	11.7		.208		.208
3	1	4.5	6.4	.080	.097	.088
	2	6.0	8.2	.108	.124	.116
	3	7.3	9.5	.129	.143	.136
	4	8.5	10.4	.151	.158	.154
	5	9.8	12.3	.175	.186	.180
	6	11.5	13.3	.205	.202	.203
	7	12.8	15.1	.228	.230	.229
	8	10.8	14.5	.192	.221	.207
4	1	4.5		.080		.080
	2	5.9		.105		.105
	3	7.0		.125		.125
	4	8.7		.154		.154
	5	10.1		.180		.180
	6	11.1		.197		.197
	7	11.8		.211		.211
	8	12.4		.221		.221
5	1	5.2	6.4	.093	.097	.095
	2	6.4	8.2	.114	.124	.119
	3	7.0	9.1	.124	.138	.131
	4	8.4	10.4	.150	.158	.154
	5	9.9	12.2	.177	.185	.181
	6	11.2	13.1	.200	.198	.199
	7	12.1	14.3	.215	.217	.216
	8	11.2	13.4	.200	.204	.202
6	1	5.2		.092		.092
	2	6.0		.107		.107
	3	7.2		.128		.128
	4	8.7		.154		.154
	5	10.0		.178		.178
	6	11.2		.200		.200
	7	12.7		.226		.226
	8	10.8		.192		.192
7	1	5.9	6.5	.106	.099	.103
	2	6.4	8.1	.114	.123	.118
	3	7.6	9.3	.136	.141	.139
	4	8.7	11.0	.155	.166	.160
	5	9.7	11.8	.172	.179	.176
	6	11.5	13.4	.205	.204	.204
	7	12.3	13.5	.219	.205	.212
	8	12.0	13.7	.214	.208	.211
8	1	5.4		.096		.096
	2	6.7		.117		.117
	3	7.9		.140		.140
	4	9.3		.165		.165
	5	10.8		.192		.192
	6	13.0		.231		.231
	7	14.3		.254		.254
	8	14.5		.258		.258
9	1	5.0	6.1	.090	.093	.092
	2	6.8	7.3	.121	.111	.116
	3	8.3	9.5	.148	.144	.146
	4	10.4	11.6	.184	.176	.180
	5	11.6	14.3	.206	.216	.211
	6	14.0	15.9	.249	.241	.245
	7	14.1	15.1	.252	.229	.240
	8	14.6	19.5	.261	.297	.279

*see note 3

Notes:

1) Row numbers refer to the vertical rows of square openings between trashrack columns, counting from the right.
2) Level numbers refer to the horizontal rows of square openings between rib arches, counting from the top.
3) Discharge and H. W. L. were set for convenience of obtaining trashrack velocities and do not necessarily agree with the tunnel rating curves.